Activity of CaMKIIa+ dorsal cochlear nucleus neurons are crucial for tinnitus perception but not for tinnitus induction

Thawann Malfatti[1], Barbara Ciralli[1], Markus M. Hilscher[2], Richardson N. Leao[1] & Katarina E. Leao[1]*

[1]Hearing and Neuronal activity Lab, Brain Institute, Federal University of Rio Grande do Norte, Natal, Brazil

[2]Institute for Analysis and Scientific Computing, Vienna University of Technology, Vienna, Austria

*katarina.leao@neuro.ufrn.br

Brain Institute, Federal University of Rio Grande do Norte, Postal box 1524 - Campus Universitário Lagoa Nova, CEP 59078-970, Natal/RN, Brasil

Abstract

The dorsal cochlear nucleus (DCN) is a region known to integrate somatosensory and auditory inputs and is identified as a potential key structure in the generation of phantom sound perception, especially noise-induced tinnitus. Yet, how altered homeostatic plasticity of the DCN induces and maintains the sensation of tinnitus is not clear. Here, we chemogenetically decrease activity of a subgroup of DCN neurons, Ca^{2+}/Calmodulin kinase 2α (CaMKIIα) positive DCN neurons, using Gi-coupled human M4 Designer Receptors Exclusively Activated by Designer Drugs (hM4Di DREADDs), to investigate their role in noise-induced tinnitus. Mice were exposed to loud noise (9-11kHz, 90dBSPL, 1h, followed by 2h of silence) and auditory brainstem responses (ABRs) and gap prepulse inhibition of acoustic startle (GPIAS) were recorded two days before and two weeks after noise exposure to identify animals with a significantly decreased inhibition of startle, indicating tinnitus but without permanent hearing loss. Neuronal activity of CaMKIIα+ neurons expressing hM4Di in the DCN was lowered by administration of clozapine-N-oxide (CNO). We found that acutely decreasing firing rate of CaMKIIα+ DCN units decrease tinnitus-like responses ($p = 0.038$, $n = 11$ mice), compared to the control group that showed no improvement in GPIAS (control virus; CaMKIIα-YFP + CNO, $p = 0.696$, $n = 7$ mice). Extracellular recordings confirmed CNO to decrease unit firing frequency of CaMKIIα-hM4Di+ mice and alter best frequency and tuning width of response to sound. However, these effects were not seen if CNO had been previously administered during the noise exposure ($n = 6$ experimental and 6 control mice). Our results suggest that CaMKIIα-hM4Di positive cells in the DCN are not crucial for tinnitus induction but play a significant role in maintaining tinnitus perception in mice.

Keywords: tinnitus, dorsal cochlear nucleus, chemogenetics, unit recording, GPIAS

1 Introduction

Noise-induced tinnitus affects 10-15% of the world population (Heller, 2003; Gallus et al., 2015), where 1-2% seek medical assistance for severely decreased quality of life due to chronic tinnitus-related irritability, stress, anxiety and/or depression (Møller, 2007; Langguth et al., 2011; Shore et al., 2016). The origin of tinnitus pathophysiology have been linked to the dorsal cochlear nucleus (DCN) of the auditory brainstem

(Kaltenbach et al., 2005; Tzounopoulos, 2008; Baizer et al., 2012; Shore et al., 2016; Shore and Wu, 2019), however, tinnitus generation and perception mechanisms are not well separated and far from completely understood.

Noise overexposure is known to alter firing properties of DCN cells (Brozoski et al., 2002; Finlayson and Kaltenbach, 2009; Pilati et al., 2012; Li et al., 2013; Manzoor et al., 2013), even after brief sound exposure at loud intensities (Gao et al., 2016). Such alterations within the DCN circuits could relay abnormal signaling to higher auditory areas and confound spontaneous firing with sensory evoked input, generating tinnitus. It has been suggested that noise-induced tinnitus is partly due to an imbalance of excitation and inhibition within the DCN (Kaltenbach and Manz, 2012; Shore et al., 2016) due to decrease in GABAergic (Middleton et al., 2011) and glycinergic activity (Wang et al., 2009) for example. On the contrary, excitatory fusiform cells have been shown to increase burst activity (Pilati et al., 2012; Wu et al., 2016) following noise overexposure. Furthermore, a shift in bimodal excitatory drive of the DCN after noise overexposure have been shown due to down-regulation of vesicular glutamate transport 1 (VGlut1; auditory-related) and up-regulation of VGlut2 (somatosensory related) proteins in the cochlear nucleus (Heeringa et al., 2018; Han et al., 2019). We have recently shown that directly manipulating activity of Ca^{2+}/Calmodulin kinase 2α (CaMKIIα) positive DCN neurons in vivo using optogenetics can have distinct effects on unit activity of the DCN, also in neurons not responding directly to neither sound or optogenetic light stimuli (Malfatti et al., 2021), highlighting how heavily interconnected the DCN circuit is (Oertel and Young, 2004). DCN circuit disruption such as bilateral electrolytic DCN lesioning in rats has shown to prevent tinnitus generation (Brozoski et al., 2011). Also, electrical stimulation of the DCN of rats can suppress tinnitus (Luo et al., 2012), and electrical high-frequency stimulation of the DCN with noise-induced tinnitus has shown to decrease tinnitus-perception during tests (van Zwieten et al., 2019). This indicates that unspecific alterations of DCN activity can decrease tinnitus induction and perception, but if the same DCN populations are involved in the two mechanisms remains to be investigated.

Here we behaviorally examine if tinnitus perception can be reduced by lowering the activity of CaMKIIα positive DCN neurons using chemogenetics. We have recently shown this promoter to be expressed by both excitatory and inhibitory DCN neurons, but with a preference for slow-firing units (Malfatti et al., 2021), presumable excitatory fusiform cells (Ochiishi et al., 1998; Oh et al., 2014). We specifically investigated if noise-induced tinnitus, without hearing loss, can be ameliorated by lowering DCN neuronal activity. Next we decrease CaMKIIα+ DCN neurons activity already during noise overexposure, to investigate if the same population is important for induction of tinnitus, and found that CaMKIIα+ DCN neurons play different roles in induction and maintenance of noise-induced tinnitus.

2 Methods

2.1 Animals

Male C57Bl/6J mice (n=30) were used at the age of 21 days at first and 2 months at the last experiment, and were used for each step of the experimental timeline (see complete timeline in Figure 7A). All animal procedures were approved and followed the guidelines of the Ethical Committee of Animal Use (CEUA) from the Federal University of Rio Grande do Norte (CEUA protocol number 051/2015). Animals were housed on a 12h/12h day/night cycle and had free access to food and water.

2.2 Gap prepulse inhibition of acoustic startle reflex

The gap prepulse inhibition of acoustic startle (GPIAS, Turner et al., 2006) test, based on the acoustic startle reflex in response to sudden loud sounds, was conducted in a sound-shielded room inside a sound-shielded chamber with LED lights. During recordings, the animal was placed inside a clear acrylic tube (Acrilart, Natal, Brasil), dimensions 6.1x5.9x5.1cm, with perforated plates closing the tube at both ends. The tube dimensions restricted mice from standing on the back paws. A speaker (Selenium Trio ST400, JBL by Harman, Brazil) was placed 4.5cm away from the restraining tube. In order to measure the animal's startle reflex, a piezoelectric or a digital accelerometer was mounted to the base plate of the restraining tube. Sound stimulus consisted of blocks of narrow-band uniform white noise at background level, loud intensity (105dBSPL) or silence. Specifically, the stimulus was presented in the following sequence: a random integer value between 12 and 22 seconds of noise at background level (randomized background noise between trials); 40ms of noise at background level for No-Gap trials, or 40ms of silence for Gap trials (Gap portion); 100ms of noise at background level (background noise before loud pulse); 50ms of noise at 105dBSPL (loud pulse); and 510ms of noise at background level (final background noise). Timestamp marks were used only for the loud pulse. The bands of frequencies tested were 8-10, 9-11, 10-12, 12-14, 14-16 and 8-18kHz. Background noise level was, for the initial GPIAS test, 60dBSPL. For GPIAS after noise exposure, background noise level was routinely adjusted to 10dBSPL above the hearing threshold for the frequency tested.

Before each session the acrylic tube was cleaned with ethanol (70%) and next with water to remove residual smell of ethanol. Animals were habituated by handling for 10 minutes in the test room for two consecutive days followed by three days of acclimatization where animals were placed in the GPIAS tube and exposed to background noise, and next returned to their homecage. A successful acclimatization and habituation was considered when animals enter freely and do not urinate or defecate in the tube. After the habituation/acclimatization period, animals were screened for gap detection capability. The animals were placed in the restraining tube and left in the recording chamber for 5 minutes, allowing the animal to stay calm and stop exploring the chamber (Valsamis and Schmid, 2011). The test consisted of 18 trials per band of frequency tested, 9 with gap (Gap trials) and 9 with noise filling the gap portion of the stimulus (No-gap trials), presented pseudo-randomly. The GPIAS sessions were carried out at 3 time points for each animal. Initially, for screening animals before being included in experimental groups (see analysis for exclusion criteria), then in the end of the experiment timeline in the following NaCl injections, and the following day 30 min after CNO (0.5mg/kg, dissolved in dimethyl sulfoxide - DMSO at 3.3mg/ml, then diluted in NaCl to the final concentration of 50μg/ml) administration. Each GPIAS session lasted between 23-41 min in total (depending on the randomization of inter pulse intervals). Upon the end of the session animals were returned to their home cage.

2.3 Virus injection

Mice were anesthetized with an i.p. injection of ketamine-xylazine combination at 90/6 mg/kg. When necessary, additional ketamine at 45 mg/kg was applied during surgery. The mouse was next mounted into a stereotaxic device resting on a heating block (37°C). The eyes were covered with dexpanthenol to prevent ocular dryness and povidone-iodine 10% was applied onto the skin of the animal's head to avoid infections. The skin was anesthetized with lidocaine hydrochloride 3% before a straight incision was made, and hydrogen peroxide 3% was applied onto the exposed skull to remove connective tissue and visualize

bone sutures. A small hole was carefully drilled at bilateral DCN coordinates (anteroposterior; AP=-6.24mm and mediolateral; ML=±2.3mm) using a dental microdrill. Next aliquoted virus (experimental: rAAV5/CaMKIIα-HA-hM4D(Gi)-IRES-mCitrine, UNC Vector Core #AV4617C, viral concentration of 1.6x10i^{12}vm/ml; or control: rAAV5/CaMKIIα-eYFP, UNC GTC Vector Core #AV4808D, 4.4x10^{12}vm/ml) was rapidly thawed and withdrawn (1.5μl) using a syringe pump (Chemyx NanoJet infusion pump). The needle (10μl Nanofil syringe with a 34-gauge removable needle) was slowly inserted into the brain (dorsoventral; DV=4.3mm) and 0.75μl of virus was infused (0.15μl/min). At completed infusion, the needle was kept in the DV coordinate for five minutes to allow for the virus to diffuse, and then the needle tip was retracted to 3.8mm DV, where 0.75μl of virus was again infused at the same rate. After the second infusion, the needle was kept in place for 10 minutes, to allow for a complete diffusion into the target area, before carefully removed. The same procedure was performed bilaterally. Following injections the skin was sutured, lidocaine hydrochloride 3% applied over the suture and 200μl of NaCl subdermally injected for rehydration. Animals were monitored until fully recovered from anesthesia.

2.4 Auditory brainstem responses

Similarly to the GPIAS setup, the speaker was connected to a sound amplifier connected to a sound card; and placed 4.5cm away from a stereotaxic frame. Field potentials (auditory brainstem responses - ABRs) were recorded using two chlorinated coiled Ag/AgCl electrodes as a recording and a reference electrode (1kΩ impedance). The electrodes were connected to the RHD2132 headstage through a DIP18-Omnetics connector, connected to Open-ephys board. Animals were anesthetized with an i.p. injection of ketamine-xylazine combination at 90/6 mg/kg and fitted to the stereotaxic frame, placed on an electric thermal pad and kept at 37°C. Dexpanthenol or NaCl was applied on the animal's eyes to avoid drying of the ocular surface. Next the scalp was disinfected with polividone-iodine (10%) and two small incisions were made: one in the skin covering the lambda region and another in the skin over the bregma region. The electrodes were placed subdermally into the incisions and the ground was connected to the system ground. The electrode at bregma was used as reference, and the electrode over lambda was used for recording. Sound stimuli consisted of narrow-band uniform white noise pulses (3ms), presented at 10Hz for 529 repetitions for each frequency and intensity tested. The frequency bands tested were the same used for GPIAS: 8-10, 9-11, 10-12, 12-14 and 14-16kHz (with exception for the 8-18kHz frequency band); and sound pulses were presented at decreasing intensities from 80 to 35dBSPL, in 5dBSPL steps, with 10s of silence between different intensities. After the test, electrodes were removed, lidocaine hydrochloride 3% was applied on the incisions and 200μl of NaCl was injected subdermally for rehydration. Animals were monitored after surgery until fully recovered from anesthesia and then returned to their home cage.

2.5 Noise exposure

Anesthetized mice were placed inside a sound-shielded chamber, inside an acrylic tube, in an acoustically shielded room, with a speaker placed 4.5cm in front of the head of the mouse. Noise exposure consisted of narrow-band uniform white noise presented at 90dBSPL, 9-11kHz, for 1 hour. The animal was left in the acrylic tube, in the sound-shielded chamber for 2h following noise exposure, since external noise following noise exposure can interfere in tinnitus development (Norena and Eggermont, 2006; Sturm et al., 2017). During noise exposure and the silence period, the animal was monitored each 15 minutes and later

returned to its homecage. Animals were given two days to recover before any further procedures. In some experiments CNO (0.5mg/kg) was given 30 min prior to noise exposure.

2.6 *in vivo* unit recording

Animals were anesthetized with an i.p. injection of ketamine-xylazine combination at 90/6 mg/kg, and placed into the stereotaxic frame similar to for ABR recordings. A small craniotomy was drilled above the left DCN (AP=-6.24mm ML=-2.3mm) and a silicon depth probe (16 channels, 25 or 50μm channel spacing, 177μm recording site area, 5mm long shank; NeuroNexus A16) dipped in fluorescent dye (1,1'-dioctadecyl-3,3,3',3'-tetramethylindocarbocyanine perchlorate; DiI, Invitrogen) for 10 minutes (for probe position) before lowered into the DCN (DV=4.3mm). A coiled Ag/AgCl wire soldered to a jumper wire was used as reference. The probe and reference wire were both connected to a headstage (RHD2132) through an adaptor (DIP18-Omnetics) connected to Open-ephys board, recording at a sampling rate of 30kHz. Sound stimulus consisted of narrow-band uniform white noise pulses (3ms) as described for ABRs, presented at 10Hz for 529 repetitions for each frequency and intensity tested. Spontaneous activity was recorded for 5 minutes, then the animal received an i.p. injection of NaCl, then sound stimulation started 30 minutes later. Subsequently, the same procedure was repeated for CNO (0.5mg/kg). At the end of the recording session the animals were either sacrificed by intracardial perfusion (20mL PBS and 20mL paraformaldehyde 4%) or by an overdose of ketamine followed by decapitation.

2.7 Data analysis

All scripts used for controlling devices, stimulation control and data analysis are available at https://gitlab.com/malfatti/LabScripts. The operating system of choice was Gentoo GNU/Linux, due to its flexible management of libraries (Ioanas, 2017). Recordings were done using Open-ephys GUI (Siegle et al., 2015). Microcontrollers and sound cards were controlled using SciScripts (Malfatti, 2020), and the sounddevice python library (Geier, 2015) was used to read and write signals from/to the sound card. Calculations were done using Scipy (Jones et al., 2001; Virtanen et al., 2020), Numpy (Van Der Walt et al., 2011; Harris et al., 2020) and SciScripts (Malfatti, 2020), and all plots were produced using Matplotlib v3.3.2 (Hunter, 2007; Caswell et al., 2020). Spikes were detected and clustered using SpyKING Circus (Yger et al., 2018; Yger and Marre, 2019), and visual inspection was performed using Phy (Rossant et al., 2016; Rossant, 2016).

GPIAS signal was bandpass filtered from 70 to 400Hz for piezoelectric recordings and lowpass filtered below 50Hz for accelerometer recordings. Data was cut 200ms around the loud pulse onset. For accelerometer recordings, the absolute values of the three axes were averaged. The 9 Gap trials of the same frequency band were averaged, as were the 9 No-gap trials. The instantaneous amplitude of the signal was calculated as the magnitude of the analytic representation of the averaged signal using the Hilbert transform. The amplitude of the response was defined as the mean instantaneous amplitude 100ms after the loud sound pulse subtracted by the mean instantaneous amplitude 100ms before the loud pulse, which corrects for baseline offsets. The GPIAS index was calculated as

$$\left(1 - \left(\frac{Gap}{NoGap}\right)\right) * 100$$

where $NoGap$ is the amplitude of response to No-gap trials and Gap is the amplitude of response to Gap

trials. The most affected frequency for each animal was calculated as the frequency with the greatest index shift from before to after noise exposure. Group data is shown as boxplots, where horizontal lines show the median, triangles show mean, circles show outliers and whiskers bounding 99% of the data points. Comparisons between treatments were done using two-tailed paired Student's t-test, Bonferroni-corrected for the number of frequency bands tested. On screening GPIAS capability before including animals into the study, animals that did not show a startle suppression of at least 30% (Li et al., 2013) in Gap vs NoGap trials for all frequencies were re-tested on the next day only on those frequencies. Animals that still did not show a startle suppression by the silent gap of at least 30% at least two frequencies were excluded from further experiments.

ABR recordings were filtered using a 4th order butterworth digital bandpass filter (600-1500Hz), and data was sliced 3ms before to 9ms after each sound pulse onset and the 529 trials were averaged. ABR peaks were detected in the highest intensity response as values one standard deviation (SD) above the mean, larger than the previous value, and larger or equal to the next value. Next, each decreasing intensity was screened for peaks where a "valid peak" follows the above criteria and, in addition, has to be preceded by a peak in the previous intensity, displaying an increased latency compared to the peak in the higher intensity response. Hearing threshold was defined as the lowest sound intensity where a peak can be detected following the above criteria. If the threshold is defined as 35dBSPL, the animal's actual hearing threshold was considered as $\leq$ 35dBSPL. As for GPIAS results, group data is shown as boxplots, where horizontal lines show the median, triangles show mean, circles show outliers and whiskers bounding 99% of the data points. Data is reported as mean $\pm$ standard error of the mean (SEM), and Student's t-test, two-tailed, unequal variance was applied to compare pairwise differences. The reported p-values were bonferroni-corrected when the same dataset was used for multiple comparisons.

Spikes from unit recordings were detected and clustered using the following parameters: 4th order butterworth digital bandpass filter from 500 to 14250Hz; detect negative spikes; single threshold from $2 \sim 4.5\times$ SD; 3 features per channel. Peri-stimulus time histograms (PSTHs) were calculated by summing occurrence of spikes in a time window of 100 ms around each TTL (50ms before and 50 ms after the TTL) and presented as number of spikes per time, where each bin corresponds to 1ms. Units were classified as responding units as described by Parras et al. (2017). Spike rate was calculated as spike events per second along all the recording (including the stimulation period). The firing rate of each unit was calculated for each frequency and intensity tested, and plotted as frequency-intensity-firing rate pseudocolor retangular grid plots, then firing rate was bilinearly interpolated, upsampling 3x in frequency and intensity dimensions. Unit tuning width was calculated as the mean of the normalized firing rate for each frequency tested at 80dB, therefore, higher values represent broader tuning curves. Unit best frequency was defined as the sound frequency that elicited the highest firing rate. Group data is reported as mean $\pm$ SEM, and paired two-tailed Student's t-test with unequal variance was applied to compare firing rate between neurons. Correlation between unit features (firing rate, tuning width and best frequency) was calculated as Pearson correlation coefficient and p-value for testing non-correlation.

3 Results

3.1 Inhibition of CaMKIIα-hM4Di positive DCN cells decreases tinnitus perception

To investigate the cellular contribution to noise-induced tinnitus mice were initially screened for capability to carry out the gap prepulse inhibition of acoustic startle (GPIAS) test developed for evaluating tinnitus in rodents (Turner et al., 2006). Mice were acclimatized and habituated to the test equipment before subjected to GPIAS (Figure 1A) testing the capability of detecting a short (40ms) silence in background noise (60dBSPL) 100ms prior to a loud startle pulse (105dBSPL, 50ms duration), thereby suppressing the acoustic startle reflex by at least 30% (Li et al., 2013). Six different frequency bands were pseudo-randomly presented with the startle pulse (no-gap session) or the silence in noise (gap session) and the startle suppression index was calculated for each frequency. Mice (P26) not showing gap-detection capabilities for at least two frequencies were excluded from further experiments (4/34 mice, 11.8%; Li et al., 2013).

Next, mice were injected bilaterally with viral vectors to transduce expression of inhibitory Designer Receptors Exclusively Activated by Designer Drugs (DREADDs; Armbruster et al., 2007) based on mutated muscarinic (M4) receptors (rAAV5/CaMKIIα-HA-hM4D(Gi)-IRES-mCitrine, or for control experiments only a fluorescent protein, rAAV5/CaMKIIα-eYFP) containing the CaMKIIα promoter, in the DCN. Mice were returned to their home cage and left approximately one month (Figure 1A) for adequate hM4Di expression in CaMKIIα expressing cells, comprising both excitatory and some inhibitory cell populations (Malfatti et al., 2021). Hearing threshold was evaluated by recording auditory brainstem responses (ABRs, Figure 1B-C) three days prior to noise exposure (1h, 90dBSPL, 9-11kHz filtered uniform white noise, followed by 2h in silence) under anesthesia in order to induce tinnitus-like behavior (Winne et al., 2020). Recording of ABRs were repeated three days after noise exposure to examine any potential hearing threshold shift (Figure 1A; Winne et al., 2020), as the aim was to study tinnitus mechanisms unrelated to persistent hearing loss. ABRs showed no significant difference in hearing threshold (hM4Di noise exposed: 41±0.9dBSPL, n = 11 mice; eYFP noise exposed: 47±1.1dBSPL; n = 7 mice, $p > 0.08$ for all frequencies tested, Figure 1C).

Next tinnitus-like perception was tested using GPIAS, with test rationale that if the animal has noise-induced tinnitus the animal will fail to perceive the silent gap (at a particular frequency), and thereby show lower gap-induced suppression of startle (Figure 1D-E). When measuring the GPIAS response after noise exposure, mice received an i.p. injection of NaCl (same volume as for CNO treatment, 10μl/g), 30 min before the test, to perform the same procedures as for when subsequently activating inhibitory DREADDs. Group data of GPIAS indices did not reveal any particular frequency more affected by noise exposure (Figure 1F, n = 18 mice, $p > 0.051$ for all frequencies), as tinnitus frequency may vary individually in animals (Coomber et al., 2014). Therefore we report the most affected frequency band, with largest change in startle suppression before and after noise exposure (Figure 1G), as parameter for tinnitus (Winne et al., 2020). Together, results showed that noise exposure induced tinnitus-like responses in mice (n = 18 mice, $p = 5.6e-09$; Figure 1H) but without a permanent hearing threshold shift.

To evaluate if lowering the activity of CaMKIIα+ DCN neurons can reduce tinnitus perception, mice received an i.p injection of low dose CNO (0.5mg/kg) 30 min prior to a repeated GPIAS test (Figure 2A). Mice injected with hM4Di showed tinnitus responses after noise exposure (NE - initial startle suppression: 80.2±2.3%; post NE with NaCl injection: 3.1±0.7%; n=11 mice, $p = 9.4e-09$) and then showed a

significant improvement in detecting the silent gap under the effect of CNO compared to NaCl (31.8±7.3%; $p = 0.038$; Figure 2B). The control group, injected with eYFP, also showed tinnitus responses after noise exposure (initial startle suppression: 67.2±12.2%; post NE with NaCl injection: 3.9±2.4%; n=7, $p = 0.016$) but no improvement was observed after CNO injection compared to NaCl (2.6±1%; $p = 0.696$, Figure 2C). This indicates that lowering the activity of CaMKIIα-hM4Di positive cells in the DCN can acutely and partially ameliorate tinnitus.

3.2 Unit recordings confirms hM4Di expressing cells decrease firing upon CNO injections

Recent work has shown CNO to not pass the blood-brain barrier (Gomez et al., 2017), instead reverting back to clozapine when administered (Jendryka et al., 2019) but with the ability to activate DREADD receptors at low concentrations avoiding off target effects (Cho et al., 2020). To assure CNO injections generated DREADD-specific effets we recorded extracellular responses from DCN units after the behavioral tests (at the end of the experimental timeline). We used short sound pulses (3ms; 8-10, 9-11, 10-12, 12-14 and 14-16kHz filtered uniform white noise) at different sound intensities (80-35dBSPL, 5dBSPL decreasing steps; presented at 10Hz) to confirm chemogenetic lowering of neuronal activity. Spontaneous (5min) and sound-evoked activity was recorded using a 16-channel single-shank silicon probe lowered into the left DCN (Malfatti et al., 2021) in response to auditory stimuli following NaCl and CNO i.p. injections (30 min prior to recordings, Figure 3A). A total of 224 units were isolated from 18 noise-exposed mice. Units were analyzed for firing rate and best frequency (frequency eliciting the maximum firing rate) in response to different narrow-band frequencies at different sound pressure levels (Figure 3B, see Table 1). Administration of CNO significantly decreased the average firing rate in hM4Di expressing animals in response to 80dBSPL at best frequency (NaCl: 15.85±1.95Hz vs. CNO: 8.96±1.53Hz, p = 1.3e-04, Figure 3C, left). Examining units from hM4Di+ mice in detail showed 96/122 units decreased firing rate (66±2% decrease in firing frequency; Figure 3C insets; Suppl. Figure S1A, middle) and 26/122 units increased firing rate following CNO administration (132±28% increase; Figure 3C insets; Suppl. Figure S1A, right). In control animals expressing eYFP, CNO injections did not significantly change the average firing rate of units (NaCl: 14.36±1.67Hz vs. CNO: 13.21±1.62Hz, n = 102 units from 7 mice, p = 0.4, Figure 3C, right). As auditory neurons are developmentally tuned to respond better to certain frequencies, we further analyzed tuning width and any change in best frequency of each unit. For tuning width, lower values represent narrower frequency response peaks. Here we found an average decrease in tuning width following CNO administration (0.78±0.01 to 0.74±0.01, p = 0.019, Figure 3D, left), but after closer examination 71/122 (58%) units decreased while 51/122 (42%) increased tuning width in response to the short sound pulses tested (Figure 3D insets; Suppl. Figure S1B). No significant changes were observed in control eYFP animals (0.67±0.01 to 0.69±0.01, p = 0.094, Figure 3D, right). Finally, we tested if units changed to what frequency they display maximum firing rate (best frequency) after CNO injection. Data showed a small but significant average increase in best frequency (12.16±0.22Hz to 12.83±0.21Hz, p = 0.026, Figure 3E, left), with 57/122 (47%) increasing, 30/122 (24%) decreasing, and 35/122 units (29%) maintaining the same best frequency for both treatments (Figure 3E insets; Suppl. Figure S1C). Taken together, electrophysiological data shows that inhibition of CaMKIIα-hM4Di positive DCN cells indeed lowers the average firing rate of DCN neurons, as well as, affecting tuning width and best frequency in the DCN circuitry, which may decrease the tinnitus perception as seen by behavioral improvement of GPIAS after CNO administration.

3.3 Decreasing CaMKIIα-hM4Di positive DCN cells activity during noise exposure does not prevent tinnitus-like behavior

As the CaMKIIα-hM4Di positive DCN cells contribute to tinnitus-like behavior, we next wanted to test if decreasing activity during noise exposure can prevent generation of noise-induced tinnitus. For this we decreased the activity of CaMKIIα-hM4Di positive DCN cells by administering CNO (0.5mg/Kg) 30 min prior to noise exposure to have a maximum effect (Guettier et al., 2009, ; Figure 4A). ABRs before and after noise exposure showed no indication of permanent hearing loss (n = 6 mice, $p > 0.08$ for all frequencies; Figure 4B-C) in this experimental condition. Furthermore, inhibition of CaMKIIα-hM4Di+ DCN neurons during noise exposure did not prevent startle suppression deficit after noise exposure compared to the initial screening (n=6 mice, $p = 5e-03$; Figure 4D-G), indicating that lowering CaMKIIα-hM4Di+ DCN cell activity could not prevent noise-induced tinnitus.

Still, we went on to test whether the beneficial effect of acutely lowering CaMKIIα-hM4Di+ DCN cell activity in mice with noise-induced tinnitus behavior remained in animals pre-treated with CNO during the noise exposure. Animals were thereby given a second dose of CNO 30 min prior to a second round of GPIAS (Figure 5A). Surprisingly, average GPIAS responses showed no improvement in tinnitus-like responses when lowering activity of CaMKIIα-hM4Di+ DCN cells that were inhibited during noise-exposure (hM4D1+ pre-NE: 67.5±6.8%; post-NE + NaCl: 5.3±2.2%; post-NE + CNO: 16.2±11.6%; $p = 5.8e-03$ for pre-NE vs. post-NE + NaCl; $p = 0.482$ for post-NE + NaCl vs. post-NE + CNO; n = 6; Figure 5B). The control group, as expected, showed tinnitus-like responses after noise exposure (n = 6 mice, $p = 0.023$) and did not show any improvement in startle suppression after the CNO i.p. injection (eYFP pre-NE: 54.9±9.6%; post-NE + NaCl: 1.2±0.7%; post-NE + CNO: 16.5±8.8%; $p = 0.023$ for pre-NE vs. post=NE + NaCl; $p = 0.175$ for post-NE + NaCl vs. post-NE + CNO; Figure 5C). Together these experiments suggest that lowering the activity of CaMKIIα-hM4Di positive DCN cells during noise exposure does not prevent tinnitus-like behavior, thereby CaMKIIα+ DCN neuron activity does not appear crucial during noise exposure for triggering tinnitus. Also, interestingly, if CaMKIIα+ DCN neurons were inhibited during noise exposure, the lowering of their activity using CNO in animals presenting noise-induced tinnitus no longer leads to the amelioration of tinnitus as seen in the group not pre-treated with CNO during noise exposure (Figures 1-3).

3.4 Lowered neuronal activity during noise exposure still renders units affected by CNO

Next we investigated if CNO administration lowered CaMKIIα-hM4Di positive DCN unit activity in animals that also received CNO *during* the noise exposure (Figure 6A). Again we compared firing frequency, tuning width and best frequency in the presence of NaCl or CNO (Figure 6B, Table 1). We found that a CNO i.p. injection led to a significant decrease in firing rate (12.5±1.1Hz to 10.7±0.9Hz; n = 85 units from 6 mice; p = 4.6e-02; Figure 6C, left) in animals expressing hM4Di, but not in control animals (4.8±0.7Hz to 4.2±0.6Hz; n = 91 units from 6 mice; p = 0.195; Figure 6C, right). Also, average unit tuning width increased (0.548±0.01 to 0.587±0.01; p = 1.09e-02; Figure 6D left) and average best frequency decreased (12.6±0.2Hz to 11.8±0.2Hz; p = 4.9e-02; Figure 6E left), while the control group, expressing only eYFP, showed no significant changes in either of the parameters (p = 0.104 and 0.113, respectively; Figures 6D and E right, Table 1). Although the average response showed a significant decrease in firing frequency

Table 1: Firing rate, tuning width and best frequency features for each experimental group (NE hM4Di+ - animals exposed to noise expressing CaMKIIα-hM4Di, n=11 mice; or NE+CNO hM4Di - animals exposed to noise under effect of CNO, expressing CaMKIIα-hM4Di, n=6 mice) and each respective control (NE eYFP - animals exposed to noise expressing CaMKIIα-eYFP, n=7 mice; or NE+CNO eYFP - animals exposed to noise under effect of CNO, expressing eYFP, n=6 mice) represented as mean ± standard error of the mean (SEM). Unit responses are further subdivided based on the applied treatment (NaCl or CNO) and on the CNO response in relation to NaCl (All - all units; Decreased and Increased - units that show a decrease or an increase in that feature under effect of CNO, respectively).

	Firing rate (Hz; mean ± SEM)					
	All		Decreased		Increased	
	NaCl	CNO	NaCl	CNO	NaCl	CNO
NE hM4Di+	15.848 ± 1.948	8.965 ± 1.526	17.452 ± 2.319	5.566 ± 1.221	9.925 ± 2.916	21.516 ± 4.819
NE eYFP	14.365 ± 1.669	13.214 ± 1.621	20.347 ± 3.039	9.231 ± 2.198	9.614 ± 1.547	16.377 ± 2.253
NE+CNO hM4Di+	9.367 ± 0.669	8.452 ± 0.604	9.902 ± 0.918	7.056 ± 0.688	8.433 ± 0.885	10.883 ± 1.084
NE+CNO eYFP	4.812 ± 0.682	4.237 ± 0.59	5.766 ± 1.092	3.232 ± 0.594	4.043 ± 0.808	5.905 ± 1.141

	Tuning width (a.u.; mean ± SEM)					
	All		Decreased		Increased	
	NaCl	CNO	NaCl	CNO	NaCl	CNO
NE hM4Di+	0.776 ± 0.012	0.744 ± 0.014	0.822 ± 0.013	0.718 ± 0.02	0.711 ± 0.02	0.78 ± 0.017
NE eYFP	0.671 ± 0.012	0.692 ± 0.013	0.709 ± 0.013	0.624 ± 0.029	0.65 ± 0.017	0.729 ± 0.009
NE+CNO hM4Di+	0.608 ± 0.012	0.63 ± 0.013	0.592 ± 0.022	0.528 ± 0.024	0.621 ± 0.013	0.694 ± 0.01
NE+CNO eYFP	0.383 ± 0.02	0.399 ± 0.019	0.423 ± 0.03	0.363 ± 0.028	0.354 ± 0.026	0.425 ± 0.026

	Best freq. (kHz; mean ± SEM)					
	All		Decreased		Increased	
	NaCl	CNO	NaCl	CNO	NaCl	CNO
NE hM4Di+	12.156 ± 0.223	12.828 ± 0.206	14.4 ± 0.234	10.533 ± 0.253	10.536 ± 0.24	14.071 ± 0.206
NE eYFP	12.369 ± 0.18	12.525 ± 0.231	13.191 ± 0.246	9.957 ± 0.208	10.936 ± 0.166	14.574 ± 0.134
NE+CNO hM4Di+	12.151 ± 0.148	11.698 ± 0.154	12.862 ± 0.197	10.0 ± 0.102	10.517 ± 0.203	13.217 ± 0.24
NE+CNO eYFP	10.871 ± 0.206	10.906 ± 0.204	12.739 ± 0.423	10.087 ± 0.212	10.107 ± 0.198	12.393 ± 0.379

upon CNO administration, the modulation appeared bidirectional with 54 unit decreasing and 31 units increasing firing rate (Figure 6C insets; Suppl. Figure 2A). Similar results were seen for tuning width (31 units decreasing and 54 units increasing, Figure 6D insets) and best frequency (39 units decreasing, 46 units increasing, Figure 6E insets, Suppl. Figure S2B-C). Interestingly, the unit firing rate from animals pre-treated with CNO during noise exposure was mostly below 40kHz in these experiments, indicating a lower sample of high frequency firing units in these animals, or that typical fast spiking units fired at a lower frequency. Also, more importantly, these results show that the lack of tinnitus-like behavior improvement in the group pre-treated with CNO during noise exposure was not due to a lack of hM4Di activation, nor due to the lack of firing changes in the DCN.

3.5 DCN units are differently modulated by DREADDs if activity was also lowered during the noise-exposure

Although CNO (0.5mg/kg) administration consistently lowered the average firing rate in animals expressing hM4Di DREADDs in DCN CaMKIIα+ neurons, the bidirectional modulation seen when looking at individual unit responses to sound after CNO administration made us question whether any correlation exist between firing rate, tuning width and best frequency in response to CNO (Table 2). Here we display the units features as 3-dimensional plots for hM4Di+ and control animals (Figure 7) that received CNO during GPIAS to ameliorate from tinnitus (Figure 7B) and from hM4Di+ and control animals receiving CNO both during the noise-exposure and during GPIAS (Figure 7C) and examined any correlation between unit parameters using Pearson correlation coefficient (r), with the p-value testing non-correlation (Table 2). We found no correlation between average firing rate and best frequency for either experimental group, suggesting that decreasing CaMKIIα-hM4Di+ cells firing rate does not alter units tuning to a certain frequency. Firing rate and tuning width appeared equally correlated in the presence of NaCl or CNO, indicating that lowering CaMKIIα-hM4Di+ cells activity using DREADDs does not decouple the existing correlation between firing rate and tuning width. However, when splitting data into units either decreasing (96/122) or increasing (26/122) firing rate in response to CNO it appears that units decreasing firing rate upon CNO administration no longer correlate with tuning width, meaning that units showing low firing rate do not necessarily have a low tuning width (Table 2; Suppl. Figure S1A-B). In experiments where CNO was given during the noise exposure we instead noted that, different from the group not pre-treated with CNO during noise exposure and from the control groups, firing rate is not correlated with tuning width. Interestingly, CNO administration during unit recordings appeared to recover this missing correlation (Table 2). This could indicate that CNO during noise-exposure can influence lateral inhibition within the DCN circuitry, since the firing rate is no longer coupled to the tuning of response to sound, for example units responding with a low firing rate but broadly to neighboring frequencies.

Interestingly CNO administration prior to noise-exposure also showed a particular loss of correlation between firing rate and tuning width in control animals, for units decreasing firing rate following CNO administration compared to NaCl. This suggests that CNO, converted to clozapine, could have small electrophysiological effects on the DCN circuitry that is not seen behaviorally nor in averaged data (Figure 6, Table 2). When investigating correlations between Tuning width and Best frequency we only observed correlations between the parameters in the groups with noise-exposure without pharmacological manipulation. The correlation between tuning width and best frequency was seen for units decreasing firing rate upon CNO administration, but for units that increased firing frequency upon CNO administration this correlation was lost. This indicates that tuning width and best frequency may have a more intricate correlation pattern, being differently affected when altering firing frequency of CaMKIIa-hM4Di+ cells. This is also shown by the fact that some units dramatically change best frequency upon CNO administration while other units do not change best frequency at all (Figure 3E and 6E). Obviously, here we are limited to detecting the best frequency to the sound stimuli given in our experimental condition, not the actual best frequency. Still we again observed a correlation between tuning width and best frequency in control animals only appearing following CNO administration. This correlation was however lost when units were divided into increasing or decreasing firing frequency following CNO administration. Still, it highlights the possibility that clozapine has small electrophysiological effects despite the very low dose CNO used in this study, and that despite group data not being significantly different for control animals, there may

Table 2: Correlation pairs of firing rate (FR), tuning width and best frequency features for each experimental group (NE hM4Di+ - animals exposed to noise expressing CaMKIIα-hM4Di, n=11 mice; or NE+CNO hM4Di - animals exposed to noise under effect of CNO, expressing CaMKIIα-hM4Di, n=6 mice) and each respective control (NE eYFP - animals exposed to noise expressing CaMKIIα-eYFP, n=7 mice; or NE+CNO eYFP - animals exposed to noise under effect of CNO, expressing eYFP, n=6 mice) represented as Pearson correlation coefficient (r) and p-value for testing non-correlation (p). Unit responses are further subdivided based on the applied treatment (NaCl or CNO) and on the firing rate change under CNO in relation to NaCl treatment (All - all units; Decreased and Increased - units that show a decrease or an increase in firing rate under effect of CNO, respectively).

Firing rate x Best freq. (r, p)

	All		Decreased FR after CNO		Increased FR after CNO	
	NaCl	CNO	NaCl	CNO	NaCl	CNO
NE hM4Di+	0.064 1.000	0.059 1.000	0.085 1.000	-0.094 1.000	-0.031 1.000	0.047 1.000
NE eYFP	0.164 0.639	0.142 1.000	0.119 1.000	0.37 0.053	0.067 1.000	-0.081 1.000
NE+CNO hM4Di+	-0.081 1.000	-0.024 1.000	0.022 1.000	-0.061 1.000	-0.323 0.058	0.007 1.000
NE+CNO eYFP	0.069 1.000	0.023 1.000	0.003 1.000	0.229 1.000	0.054 1.000	-0.224 1.000

Firing rate x Tuning width (r, p)

	All		Decreased FR after CNO		Increased FR after CNO	
	NaCl	CNO	NaCl	CNO	NaCl	CNO
NE hM4Di+	0.479 2.2e-07*	0.352 6.1e-04*	0.504 1.5e-06*	0.264 0.083	0.413 0.324	0.484 0.108
NE eYFP	0.378 1.6e-04*	0.445 2.5e-06*	0.557 1.1e-04*	0.47 3.0e-03*	0.349 3.2e-02*	0.429 2.3e-03*
NE+CNO hM4Di+	0.045 1.000	0.246 5.3e-03*	0.099 1.000	0.293 9.9e-03*	-0.109 1.000	0.14 1.000
NE+CNO eYFP	0.47 5.0e-05*	0.481 2.9e-05*	0.469 1.1e-02*	0.39 0.074	0.492 2.4e-02*	0.596 1.4e-03*

Tuning width X Best freq. (r, p)

	All		Decreased FR after CNO		Increased FR after CNO	
	NaCl	CNO	NaCl	CNO	NaCl	CNO
NE hM4Di+	0.301 6.7e-03*	0.352 6.3e-04*	0.201 0.45	0.314 1.6e-02*	0.591 1.4e-02*	0.249 1.000
NE eYFP	0.198 0.252	0.252 4.7e-02*	0.182 1.000	0.138 1.000	0.247 0.378	0.263 0.27
NE+CNO hM4Di+	0.069 1.000	0.137 0.522	0.064 1.000	0.108 1.000	0.086 1.000	0.181 1.000
NE+CNO eYFP	0.068 1.000	0.231 0.306	-0.11 1.000	0.365 0.126	0.223 1.000	0.036 1.000

be small membrane effects through binding of clozapine to certain receptors - effects that are not seen when clozapine's main effect is activating DREADDs. Finally, we did not record from units of either experimental group (noise-exposed or noise-exposed + CNO) at any particular depth or layer, as we did not want to bias data to any particular region of the DCN (Figure 8). Unit recordings describes units responding to sound when CaMKIIα+ neurons of the DCN circuit had the firing frequency in response to sound chemogenetically lowered, and does thus not reflect recordings from CaMKIIα+ units only (Malfatti et al., 2021).

4 Discussion

Here we found that decreasing activity of CaMKIIα-hM4Di positive DCN cells after noise exposure can decrease tinnitus-like responses. Moreover, this subpopulation do not appear to have an important role in triggering tinnitus, since inhibiting CaMKIIα-hM4Di positive DCN cells during noise exposure did not prevent tinnitus-like responses development, and also abolished CNO-dependent recovery after noise exposure.

To not confound mechanisms of noise-induced tinnitus with plasticity related to hearing loss, auditory brainstem responses were recorded to verify that our noise exposure would not induce permanent hearing loss. Parameters for noise exposure in animal models of noise-induced tinnitus are not consistent and therefore hard to compare results between. For example, intensities can vary from 92 to 124dBSPL, noise frequencies reported range from pure tones or filtered white noise to broadband noise, and durations vary from 0.5 to 4h, some with multiple exposures, and can be unilateral or bilateral (see Bauer and Brozoski, 2001; Heffner and Harrington, 2002; Basta and Ernest, 2004; Kujawa and Liberman, 2009; Wu et al., 2016; Yang et al., 2016; Heeringa et al., 2018; Han et al., 2019; van Zwieten et al., 2019). Furthermore, the GPIAS method for tinnitus assessment has also been adopted with slightly different parameters (Galazyuk and Hébert, 2015). Also, genetic differences between mouse strains have shown differences in acoustic startle reflex, specifically related to the ability to detect a prepulse or silent gap with different inter-stimulus interval to a loud pulse (Yu et al., 2016). Here we aim to induce tinnitus without permanent hearing loss, so we used a 90dBSPL, 9-11kHz, 1h exposure followed by 2h of silence. We found that, at these parameters, tinnitus can be induced without permanent threshold shifts. Similarly to data shown by Coomber et al. (2014) from guinea pigs, we found no generalized deficit in GPIAS responses in any particular frequency. Instead, individual animals showed tinnitus responses at different frequencies, even providing the same noise exposure to all animals (Longenecker and Galazyuk, 2016).

It is known that the DCN circuitry present altered firing following noise exposure. DCN cells, specially fusiform cells, can increase spontaneous activity (Baizer et al., 2012), bursting activity and synchrony (Wu et al., 2016). Still, it is not established that tinnitus plasticity is induced during the noise exposure. Therefore lowering DCN activity during the noise exposure might not affect plasticity taking place several hours after the noise-exposure, when CNO has broken down. CNO has a half-life of 2h in mice, with biological effects lasting 6-10h (Guettier et al., 2009). Therefore we can only state that decreasing the activity of CaMKIIα-hM4Di positive DCN subpopulation during the tinnitus induction protocol does not appear to counteract the overall increased auditory activity of the auditory system enough to prevent tinnitus in mice. Moreover, DREADDs of the inhibitory type, hM4Di, belongs to G-protein coupled signaling that leads to a reduction in adenylyl cyclase, consequently decreasing cAMP production and Protein Kinase A activation, and the $G_{\beta\gamma}$ subunit opens inwardly rectifying potassium channels, inducing hyperpolarization (Rogan and Roth, 2011). How long these effects persist and potential downstream targets were not assessed in this study, and additional studies with CNO administration over longer periods following tinnitus induction would be interesting to evaluate.

One interesting indirect finding of this study was that if CaMKIIα-hM4Di positive DCN cells have a role in tinnitus triggering, they are not the only subpopulation involved, since inhibiting them is not enough to prevent tinnitus. Here, mice still develop tinnitus behavior, but since the CaMKIIα-hM4Di positive DCN cells were inhibited during noise exposure, we can speculate that no plasticity took place in those cells, and they would not collaborate to the abnormal signaling in the DCN. Thereby, inhibiting those

cells later in the GPIAS test did not improve the tinnitus perception. This would explain the fact that mice that recovered after CNO injection in the first set of experiments presented only a partial recovery (Figure 2B), meaning the startle suppression was not restored to pre-noise exposure values, but significantly improved compared to post-noise exposure after NaCl injection. It is also important to point out that we are only targeting a small area of the DCN using our electrode shank, as well as the virus injections being local and might only affect neurons in the vicinity of the injection sites (Malfatti et al., 2021). Here we could not confirm hM4Di spread of infection due to the weak expression of the mCitrine fluorescent protein. Despite these spatial limitations we were able to identify behavioral changes and record from a relatively large number of units that were affected by CNO/clozapine. Future studies using transgenic animals, with a more homogenic expression of distinct promoters coupled to cre recombinase expression (for example using cre-dependent hM4Di) may further clarify subpopulations of the DCN that are important for tinnitus induction and perception.

Recent studies have shown that clozapine-N-oxide cannot cross the blood-brain barrier, therefore being reverted to the antipsycotic compound clozapine, that binds to a large variety of neurotransmitter receptors (Gomez et al., 2017). Still, Manvich et al. (2018) showed that the amount of CNO necessary to cause behavioral changes in mice or rats is 5mg/kg, which is 10x greater than the dose administered in this study. Furthermore, we observed no changes in GPIAS responses of animals not expressing the hM4Di receptor. Data shows that CNO caused no significant changes in GPIAS responses or firing of DCN units of eYFP (control) animals. Here we found that inhibiting CaMKIIα-hM4Di positive DCN cells changed firing features of most of the recorded units. Also, even though CNO caused a significant decrease in DCN units firing rate, some units showed an increase in firing rate instead. Since hM4Di leads to cell hyperpolarization, probably some CaMKIIα-hM4Di positive DCN cells are inhibitory, then, units showing an increase in firing rate after CNO injection are most likely being disinhibited. Also there were units increasing and units decreasing its best frequency, while others did not change its best frequency. Importantly, the stimulus used during units recordings was 3ms long, 2kHz-wide narrow-band uniform noise ranging from 8 to 16kHz. This means that what we defined as best frequency and tuning-width is relative to the provided stimulus, since DCN cells may have their best frequencies at frequencies much higher than 16kHz, and respond differently to pure-tone pulses even if that particular frequency is within the noise band (Godfrey et al., 1975; Nelken and Young, 1994). For some cells, it is possible that their best frequencies are much higher than 16kHz, and could have been erroneously classified, for example, as a unit with a low firing rate and broad tuning width. Thereby we cannot state anything related to tonotopicity of the DCN in this study.

Due to the bimodal responses seen upon inhibiting CaMKIIα-hM4Di positive DCN cells, we investigated correlations between features also separated by decrease or increase of activity following CNO. We found that, in noise-exposed animals, firing rate is not correlated with best frequency, regardless of CaMKIIα-hM4Di positive DCN cells being inhibited. We found, however, that firing rate is correlated with tuning width, except for animals where CaMKIIα-hM4Di positive DCN cells were inhibited during noise-exposure. Injecting CNO 30min before sound stimulation apparently restored this correlation. Tuning width was correlated to best frequency only for the group that expressed CaMKIIα-hM4Di and did not receive CNO during noise exposure. Surprisingly, units recorded from the control group expressing CaMKIIα-eYFP that did not receive CNO during noise exposure showed no correlation between tuning width and best frequency under effect of NaCl, but showed a significant correlation between those features under effect of CNO. This shows that even though CNO caused no behavioral changes in control animals neither significant changes in

the group electrophysiological responses, some CNO is likely being metabolized back to clozapine (Gomez et al., 2017) and having off-target effects that are small enough to not significantly alter the animal's behavior or group electrophysiological responses, but that may change the circuitry dynamics such as coupling tuning width and best frequency. Put together, those results illustrate the complexity of the DCN circuitry and indicate that decreasing CaMKIIα-hM4Di positive DCN cells activity may change drastically the DCN circuitry physiology, and those changes may be underlying the improvement observed in tinnitus. Whether such changes could lead to an altered perception of tinnitus also in humans would be very interesting as one of the neurological treatment effects on tinnitus is a decreased loudness and/or annoyance index (Lefaucheur et al., 2017, 2020). In conclusion, our results show that CaMKIIα-hM4Di positive DCN cells have an important role in noise-induced tinnitus in mice. Elucidating the role of subpopulations in specific tinnitus mechanisms could allow for development of preventive and curative strategies with focus on genetic identity of certain DCN cells.

Conflict of Interest Statement

The authors declare that the research was conducted in the absence of any commercial or financial relationships that could be construed as a potential conflict of interest.

Author Contributions

TM and BC performed the experiments; TM and MH analyzed the data; TM, BC and KEL wrote the manuscript with input from RNL.

Funding

This work is supported by the American Tinnitus Association and the Brazilian National Council for Scientific and Technological Development

Acknowledgments

We would like to thank Dr. Helton Maia, Dr. George Nascimento and Dr. João Bacelo for technical advice.

Data Availability Statement

The datasets generated and/or analyzed in the current study are available on request.

References

Armbruster, B. N., Li, X., Pausch, M. H., Herlitze, S., and Roth, B. L. (2007). Evolving the lock to fit the key to create a family of g protein-coupled receptors potently activated by an inert ligand. *Proceedings of the National Academy of Sciences* 104, 5163–5168. doi:10.1073/pnas.0700293104

Baizer, J. S., Manohar, S., Paolone, N. A., Weinstock, N., and Salvi, R. J. (2012). Understanding tinnitus: The dorsal cochlear nucleus, organization and plasticity. *Brain Research* 1485, 40–53. doi: 10.1016/j.brainres.2012.03.044

Basta, D. and Ernest, A. (2004). Noise-induced changes of neuronal spontaneous activity in mice inferior colliculus brain slices. *Neuroscience Letters* 368, 297–302. doi:10.1016/j.neulet.2004.07.030

Bauer, C. A. and Brozoski, T. J. (2001). Assessing tinnitus and prospective tinnitus therapeutics using a psychophysical animal model. *Journal of the Association for Research in Otolaryngology* 2, 54–64. doi:10.1007/s101620010030

Brozoski, T. J., Bauer, C. A., and Caspary, D. M. (2002). Elevated fusiform cell activity in the dorsal cochlear nucleus of chinchillas with psychophysical evidence of tinnitus. *The Journal of Neuroscience* 22, 2383–2390. doi:10.1523/jneurosci.22-06-02383.2002

Brozoski, T. J., Wisner, K. W., Sybert, L. T., and Bauer, C. A. (2011). Bilateral dorsal cochlear nucleus lesions prevent acoustic-trauma induced tinnitus in an animal model. *Journal of the Association for Research in Otolaryngology* 13, 55–66. doi:10.1007/s10162-011-0290-3

[Dataset] Caswell, T. A., Droettboom, M., Lee, A., Hunter, J., de Andrade, E. S., Firing, E., et al. (2020). matplotlib/matplotlib: Rel: v3.3.2. doi:10.5281/zenodo.4030140

Cho, J., Ryu, S., Lee, S., Kim, J., and Kim, H.-I. (2020). Optimizing clozapine for chemogenetic neuromodulation of somatosensory cortex. *Scientific Reports* 10. doi:10.1038/s41598-020-62923-x

Coomber, B., Berger, J. I., Kowalkowski, V. L., Shackleton, T. M., Palmer, A. R., and Wallace, M. N. (2014). Neural changes accompanying tinnitus following unilateral acoustic trauma in the guinea pig. *European Journal of Neuroscience* 40, 2427–2441. doi:10.1111/ejn.12580

Finlayson, P. G. and Kaltenbach, J. A. (2009). Alterations in the spontaneous discharge patterns of single units in the dorsal cochlear nucleus following intense sound exposure. *Hearing Research* 256, 104–117. doi:10.1016/j.heares.2009.07.006

Galazyuk, A. and Hébert, S. (2015). Gap-prepulse inhibition of the acoustic startle reflex (GPIAS) for tinnitus assessment: Current status and future directions. *Frontiers in Neurology* 6. doi:10.3389/fneur.2015.00088

Gallus, S., Lugo, A., Garavello, W., Bosetti, C., Santoro, E., Colombo, P., et al. (2015). Prevalence and determinants of tinnitus in the italian adult population. *Neuroepidemiology* 45, 12–19

Gao, Y., Manzoor, N., and Kaltenbach, J. (2016). Evidence of activity-dependent plasticity in the dorsal cochlear nucleus, in vivo, induced by brief sound exposure. *Hearing research* 341, 31–42

[Dataset] Geier, M. (2015). Sounddevice. https://pypi.org/project/sounddevice/

Godfrey, D. A., Kiang, N. Y. S., and Norris, B. E. (1975). Single unit activity in the posteroventral cochlear nucleus of the cat. *The Journal of Comparative Neurology* 162, 247–268. doi:10.1002/cne.901620206

Gomez, J. L., Bonaventura, J., Lesniak, W., Mathews, W. B., Sysa-Shah, P., Rodriguez, L. A., et al. (2017). Chemogenetics revealed: Dreadd occupancy and activation via converted clozapine. *Science* 357, 503–507. doi:10.1126/science.aan2475

Guettier, J.-M., Gautam, D., Scarselli, M., de Azua, I. R., Li, J. H., Rosemond, E., et al. (2009). A chemical-genetic approach to study g protein regulation of β cell function in vivo. *Proceedings of the National Academy of Sciences* 106, 19197–19202

Han, K., Mun, S., Sohn, S., Piao, X., Park, I., and Chang, M. (2019). Axonal sprouting in the dorsal cochlear nucleus affects gap-prepulse inhibition following noise exposure. *International Journal of Molecular Medicine* doi:10.3892/ijmm.2019.4316

Harris, C. R., Millman, K. J., van der Walt, S. J., Gommers, R., Virtanen, P., Cournapeau, D., et al. (2020). Array programming with NumPy. *Nature* 585, 357–362. doi:10.1038/s41586-020-2649-2

Heeringa, A. N., Wu, C., Chung, C., West, M., Martel, D., Liberman, L., et al. (2018). Glutamatergic projections to the cochlear nucleus are redistributed in tinnitus. *Neuroscience* 391, 91–103. doi:10.1016/j.neuroscience.2018.09.008

Heffner, H. E. and Harrington, I. A. (2002). Tinnitus in hamsters following exposure to intense sound. *Hearing Research* 170, 83–95. doi:10.1016/s0378-5955(02)00343-x

Heller, A. J. (2003). Classification and epidemiology of tinnitus. *Otolaryngologic Clinics of North America* 36, 239–248

Hunter, J. D. (2007). Matplotlib: A 2d Graphics Environment. *Computing in Science & Engineering* 9, 90–95. doi:10.1109/MCSE.2007.55

Ioanas, H.-I. (2017). Gentoo linux for neuroscience-a replicable, flexible, scalable, rolling-release environment that provides direct access to development software. *Research Ideas and Outcomes* 3, e12095

Jendryka, M., Palchaudhuri, M., Ursu, D., van der Veen, B., Liss, B., KÃ¤tzel, D., et al. (2019). Pharmacokinetic and pharmacodynamic actions of clozapine-n-oxide, clozapine, and compound 21 in DREADD-based chemogenetics in mice. *Scientific Reports* 9. doi:10.1038/s41598-019-41088-2

Jones, E., Oliphant, T., and Peterson, P. (2001). SciPy: Open source scientific tools for Python. *W eb http://www. scipy. org*

Kaltenbach, J. A. and Manz, R. (2012). The neurobiology of noise-induced tinnitus. In *Noise-induced hearing loss* (Springer). 151–175

Kaltenbach, J. A., Zhang, J., and Finlayson, P. (2005). Tinnitus as a plastic phenomenon and its possible neural underpinnings in the dorsal cochlear nucleus. *Hearing research* 206, 200–226

Kujawa, S. G. and Liberman, M. C. (2009). Adding insult to injury: Cochlear nerve degeneration after "temporary" noise-induced hearing loss. *Journal of Neuroscience* 29, 14077–14085. doi:10.1523/jneurosci.2845-09.2009

Langguth, B., Landgrebe, M., Kleinjung, T., Sand, G. P., and Hajak, G. (2011). Tinnitus and depression. *The World Journal of Biological Psychiatry* 12, 489–500. doi:10.3109/15622975.2011.575178

Lefaucheur, J.-P., Aleman, A., Baeken, C., Benninger, D. H., Brunelin, J., Lazzaro, V. D., et al. (2020). Evidence-based guidelines on the therapeutic use of repetitive transcranial magnetic stimulation (rTMS): An update (2014–2018). *Clinical Neurophysiology* 131, 474–528. doi:10.1016/j.clinph.2019.11.002

Lefaucheur, J.-P., Antal, A., Ayache, S. S., Benninger, D. H., Brunelin, J., Cogiamanian, F., et al. (2017). Evidence-based guidelines on the therapeutic use of transcranial direct current stimulation (tDCS). *Clinical Neurophysiology* 128, 56–92. doi:10.1016/j.clinph.2016.10.087

Li, S., Choi, V., and Tzounopoulos, T. (2013). Pathogenic plasticity of kv7.2/3 channel activity is essential for the induction of tinnitus. *Proceedings of the National Academy of Sciences* 110, 9980–9985. doi:10.1073/pnas.1302770110

Longenecker, R. J. and Galazyuk, A. V. (2016). Variable effects of acoustic trauma on behavioral and neural correlates of tinnitus in individual animals. *Frontiers in Behavioral Neuroscience* 10. doi:10.3389/fnbeh.2016.00207

Luo, H., Zhang, X., Nation, J., Pace, E., Lepczyk, L., and Zhang, J. (2012). Tinnitus suppression by electrical stimulation of the rat dorsal cochlear nucleus. *Neuroscience Letters* 522, 16–20. doi:10.1016/j.neulet.2012.05.072

[Dataset] Malfatti, T. (2020). sciscripts. doi:10.5281/zenodo.4045873

Malfatti, T., Ciralli, B., Hilscher, M. M., Edwards, S. J., Kullander, K., Leao, R. N., et al. (2021). Using cortical neuron markers to target cells in the dorsal cochlear nucleus. *eneuro* , ENEURO.0413–20.2020doi:10.1523/eneuro.0413-20.2020

Manvich, D. F., Webster, K. A., Foster, S. L., Farrell, M. S., Ritchie, J. C., Porter, J. H., et al. (2018). The DREADD agonist clozapine n-oxide (CNO) is reverse-metabolized to clozapine and produces clozapine-like interoceptive stimulus effects in rats and mice. *Scientific Reports* 8. doi:10.1038/s41598-018-22116-z

Manzoor, N., Gao, Y., Licari, F., and Kaltenbach, J. (2013). Comparison and contrast of noise-induced hyperactivity in the dorsal cochlear nucleus and inferior colliculus. *Hearing Research* 295, 114–123. doi:10.1016/j.heares.2012.04.003

Middleton, J. W., Kiritani, T., Pedersen, C., Turner, J. G., Shepherd, G. M. G., and Tzounopoulos, T. (2011). Mice with behavioral evidence of tinnitus exhibit dorsal cochlear nucleus hyperactivity because of decreased GABAergic inhibition. *Proceedings of the National Academy of Sciences* 108, 7601–7606. doi:10.1073/pnas.1100223108

Møller, A. R. (2007). Tinnitus: presence and future. *Tinnitus: Pathophysiology and Treatment* , 3–16doi:10.1016/s0079-6123(07)66001-4

Nelken, I. and Young, E. D. (1994). Two separate inhibitory mechanisms shape the responses of dorsal cochlear nucleus type iv units to narrowband and wideband stimuli. *Journal of Neurophysiology* 71, 2446–2462. doi:10.1152/jn.1994.71.6.2446

Norena, A. J. and Eggermont, J. J. (2006). Enriched acoustic environment after noise trauma abolishes neural signs of tinnitus. *NeuroReport* 17, 559–563. doi:10.1097/00001756-200604240-00001

Ochiishi, T., Yamauchi, T., and Terashima, T. (1998). Regional differences between the immunohistochemical distribution of ca2+/calmodulin-dependent protein kinase ii α and β isoforms in the brainstem of the rat. *Brain Research* 790, 129–140. doi:10.1016/s0006-8993(98)00058-4

Oertel, D. and Young, E. D. (2004). What's a cerebellar circuit doing in the auditory system? *Trends in Neurosciences* 27, 104–110. doi:10.1016/j.tins.2003.12.001

Oh, S. W., Harris, J. A., Ng, L., Winslow, B., Cain, N., Mihalas, S., et al. (2014). A mesoscale connectome of the mouse brain. *Nature* 508, 207–214. doi:10.1038/nature13186

Parras, G. G., Nieto-Diego, J., Carbajal, G. V., Valdés-Baizabal, C., Escera, C., and Malmierca, M. S. (2017). Neurons along the auditory pathway exhibit a hierarchical organization of prediction error. *Nature communications* 8, 2148

Pilati, N., Large, C., Forsythe, I. D., and Hamann, M. (2012). Acoustic over-exposure triggers burst firing in dorsal cochlear nucleus fusiform cells. *Hearing Research* 283, 98–106. doi:10.1016/j.heares.2011.10.008

Rogan, S. C. and Roth, B. L. (2011). Remote control of neuronal signaling. *Pharmacological Reviews* 63, 291–315. doi:10.1124/pr.110.003020

[Dataset] Rossant, C. (2016). Phy. https://pypi.org/project/phy/

Rossant, C., Kadir, S. N., Goodman, D. F. M., Schulman, J., Hunter, M. L. D., Saleem, A. B., et al. (2016). Spike sorting for large, dense electrode arrays. *Nature Neuroscience* 19, 634–641. doi:10.1038/nn.4268

Shore, S. E., Roberts, L. E., and Langguth, B. (2016). Maladaptive plasticity in tinnitus — triggers, mechanisms and treatment. *Nature Reviews Neurology* 12, 150–160. doi:10.1038/nrneurol.2016.12

Shore, S. E. and Wu, C. (2019). Mechanisms of noise-induced tinnitus: Insights from cellular studies. *Neuron* 103, 8–20. doi:10.1016/j.neuron.2019.05.008

Siegle, J. H., Hale, G. J., Newman, J. P., and Voigts, J. (2015). Neural ensemble communities: open-source approaches to hardware for large-scale electrophysiology. *Current Opinion in Neurobiology* 32, 53–59. doi:10.1016/j.conb.2014.11.004

Sturm, J. J., Zhang-Hooks, Y.-X., Roos, H., Nguyen, T., and Kandler, K. (2017). Noise trauma-induced behavioral gap detection deficits correlate with reorganization of excitatory and inhibitory local circuits in the inferior colliculus and are prevented by acoustic enrichment. *Journal of Neuroscience* 37, 6314–6330

Turner, J. G., Brozoski, T. J., Bauer, C. A., Parrish, J. L., Myers, K., Hughes, L. F., et al. (2006). Gap detection deficits in rats with tinnitus: A potential novel screening tool. *Behavioral Neuroscience* 120, 188–195. doi:10.1037/0735-7044.120.1.188

Tzounopoulos, T. (2008). Mechanisms of synaptic plasticity in the dorsal cochlear nucleus: Plasticity-induced changes that could underlie tinnitus. *American Journal of Audiology* 17. doi:10.1044/1059-0889(2008/07-0030)

Valsamis, B. and Schmid, S. (2011). Habituation and prepulse inhibition of acoustic startle in rodents. *Journal of Visualized Experiments* doi:10.3791/3446

Van Der Walt, S., Colbert, S. C., and Varoquaux, G. (2011). The NumPy array: a structure for efficient numerical computation. *Computing in Science & Engineering* 13, 22

van Zwieten, G., Jahanshahi, A., van Erp, M. L., Temel, Y., Stokroos, R. J., Janssen, M. L. F., et al. (2019). Alleviation of tinnitus with high-frequency stimulation of the dorsal cochlear nucleus: A rodent study. *Trends in Hearing* 23, 233121651983508. doi:10.1177/2331216519835080

Virtanen, P., Gommers, R., Oliphant, T. E., Haberland, M., Reddy, T., Cournapeau, D., et al. (2020). SciPy 1.0: Fundamental Algorithms for Scientific Computing in Python. *Nature Methods* 17, 261–272. doi:10.1038/s41592-019-0686-2

Wang, H., Brozoski, T. J., Turner, J. G., Ling, L., Parrish, J. L., Hughes, L. F., et al. (2009). Plasticity at glycinergic synapses in dorsal cochlear nucleus of rats with behavioral evidence of tinnitus. *Neuroscience* 164, 747–759

Winne, J., Boerner, B. C., Malfatti, T., Brisa, E., Doerl, J., Nogueira, I., et al. (2020). Anxiety-like behavior induced by salicylate depends on age and can be prevented by a single dose of 5-MeO-DMT. *Experimental Neurology* 326, 113175. doi:10.1016/j.expneurol.2020.113175

Wu, C., Martel, D. T., and Shore, S. E. (2016). Increased synchrony and bursting of dorsal cochlear nucleus fusiform cells correlate with tinnitus. *The Journal of Neuroscience* 36, 2068–2073. doi:10.1523/jneurosci.3960-15.2016

Yang, H., Xiong, H., Ou, Y., Xu, Y., Pang, J., Lai, L., et al. (2016). Effect of repetitive transcranial magnetic stimulation on auditory function following acoustic trauma. *Neurological Sciences* 37, 1511–1516. doi:10.1007/s10072-016-2603-0

[Dataset] Yger, P. and Marre, O. (2019). Spyking circus. https://pypi.org/project/spyking-circus/

Yger, P., Spampinato, G. L., Esposito, E., Lefebvre, B., Deny, S., Gardella, C., et al. (2018). A spike sorting toolbox for up to thousands of electrodes validated with ground truth recordings in vitro and in vivo. *Elife* 7, e34518

Yu, H., Patil, K. V., Han, C., Fabella, B., Canlon, B., Someya, S., et al. (2016). GLAST deficiency in mice exacerbates gap detection deficits in a model of salicylate-induced tinnitus. *Frontiers in Behavioral Neuroscience* 10. doi:10.3389/fnbeh.2016.00158

Figures

672

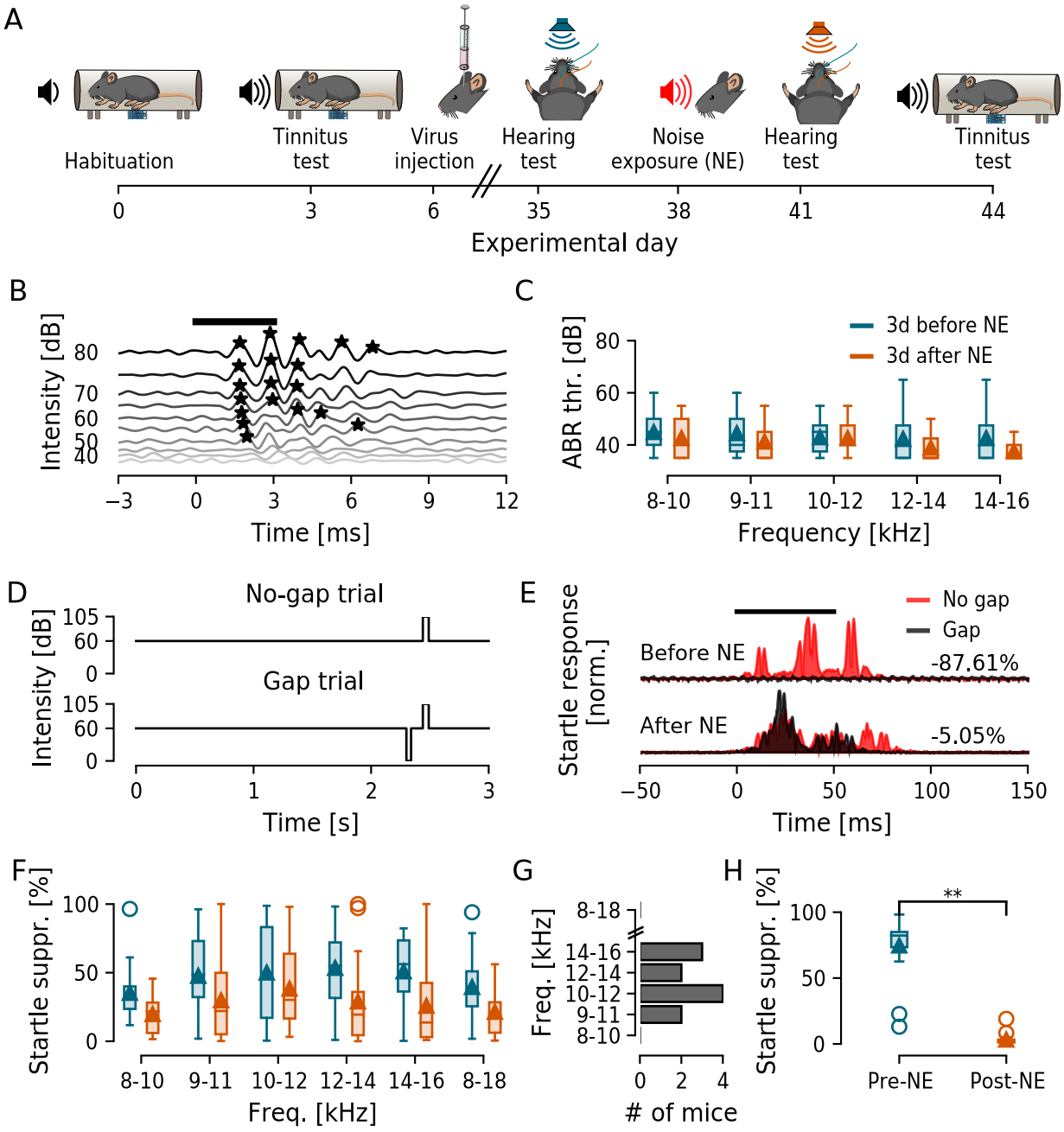

Figure 1: Noise exposure induces tinnitus without causing hearing loss. A) Experimental timeline. B) ABR representative example for 8-10kHz frequency presented from 80 to 35dBSPL. Response peaks are marked with black asterisks. The animal's hearing threshold for this frequency was defined at the last intensity with an identified peak, in this example, 50dBSPL. C) Group hearing thresholds for each frequency tested before (blue) and after (orange) noise exposure (NE). D) Schematic drawn of the gap and no-gap protocols. E) Representative GPIAS recording of a mouse showing 87.6% suppression of acoustic startle before and 5.1% suppression after noise exposure when comparing no-gap (red) and gap (black) responses, indicating tinnitus-like behaviour for the tested frequency (9-11kHz). F) GPIAS group performance before (blue) and after (orange) noise exposure. G) Histogram showing the number of animals in function of the frequency with the greatest decrease in GPIAS performance. H) GPIAS group performance at the most affected frequency of each animal (n = 18 mice). **: p = 5.6e-09.

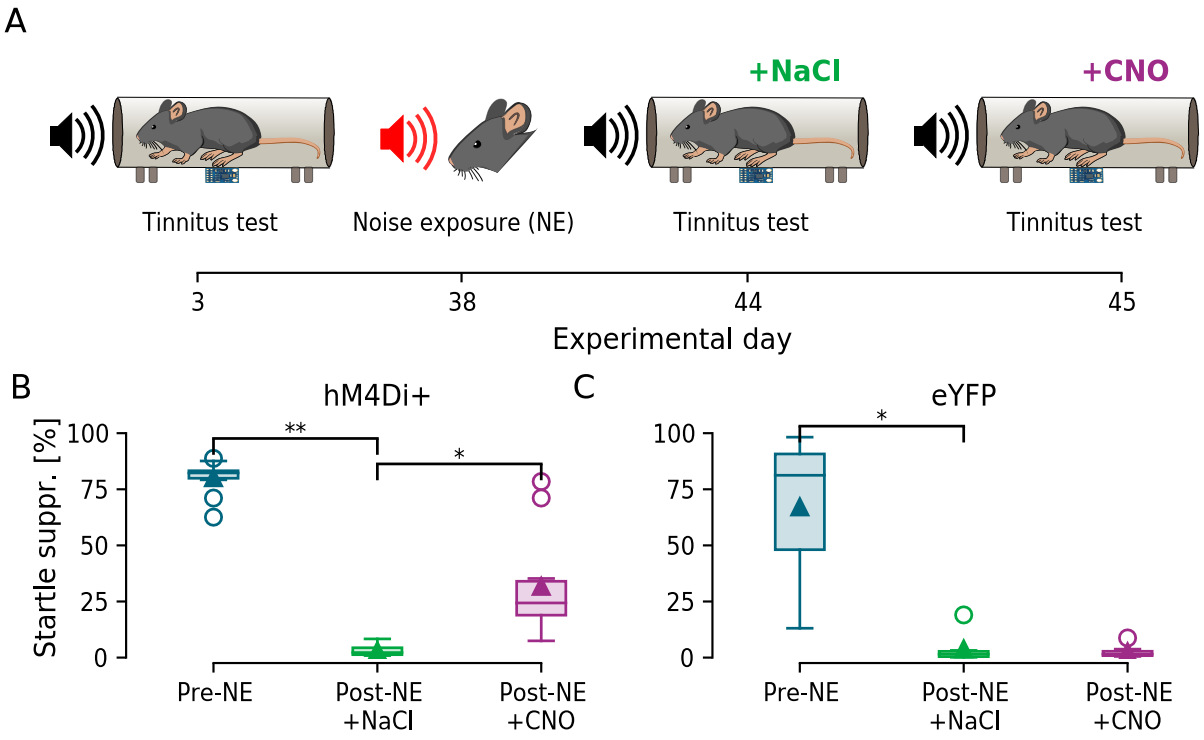

Figure 2: Inhibition of DCN CaMKIIα-hM4Di positive cells after noise exposure decreases tinnitus-like behaviour. A) Schematic GPIAS recordings timeline. B) GPIAS group performance showing that animals expressing CaMKIIα-hM4Di decrease startle supression after noise exposure (n = 11 mice) and increase startle supression when under the effect of CNO. C) GPIAS control group performance (expressing enhanced yellow fluorescent protein, eYFP) showing that although presenting tinnitus-like responses after noise exposure (n = 7 mice) no difference can be observed between NaCl and CNO treatments ($p = 0.696$). *: $p < 0.05$; **: $p = 9.4e\text{-}09$.

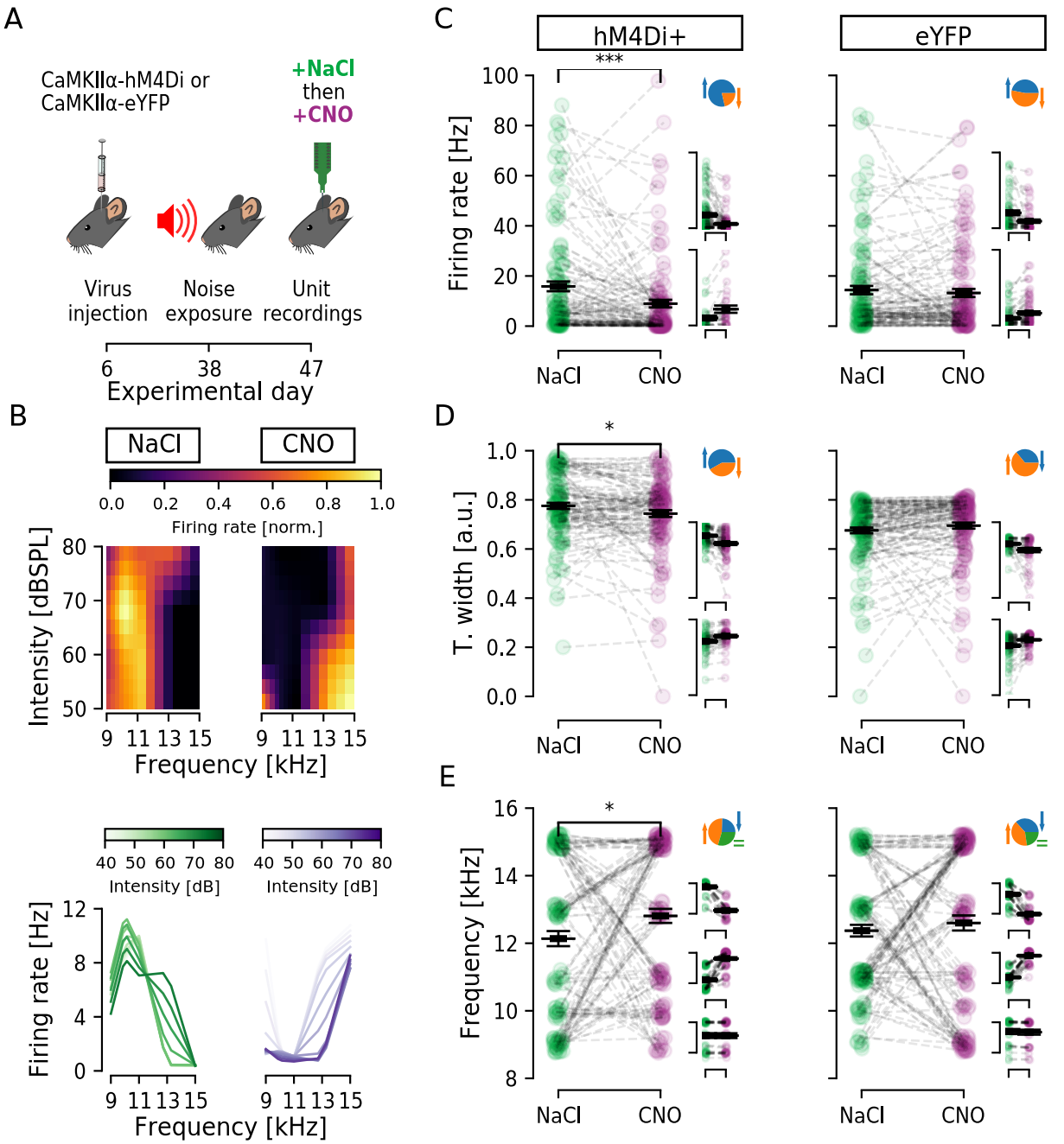

Figure 3: Decreasing CaMKIIα-hM4Di positive cells activity in the DCN changes firing properties of the circuitry. A) Timeline of experiments highlighting viral injection, noise exposure and unit recordings. B) Top, firing rate (colormap) of a representative unit after NaCl (left) and CNO (right) for each intensity (lines) and each frequency (columns) tested. Bottom, a different representation of the same representative examples in the top, showing firing rate per frequency for each intensity. Data was upsampled 3 times in the intensity and frequency dimensions. C-E) Units firing rate (C), tuning width (D) and best frequency (E) for stimulation at 80dBSPL, at each unit best frequency (n = 11 mice, 122 units). Animals expressing hM4Di (left) showed a significant decrease in firing rate (C), decrease in tuning width (D) and increase in best frequency (E). Control animals expressing eYFP (right) showed no significant change in any of those parameters. Individual unit values are shown in green (NaCl) or purple (CNO) condition. Black line indicates mean ± SEM. Insets C-E (top) shows portion of units decreasing (blue) and increasing (orange) values upon CNO administration. Inset (bottom) shows distribution of unit values divided in groups for decrease, increase or no change (for larger representation see Suppl. Figure S1). *: $p < 0.05$; ***: $p = 1.3e\text{-}04$.

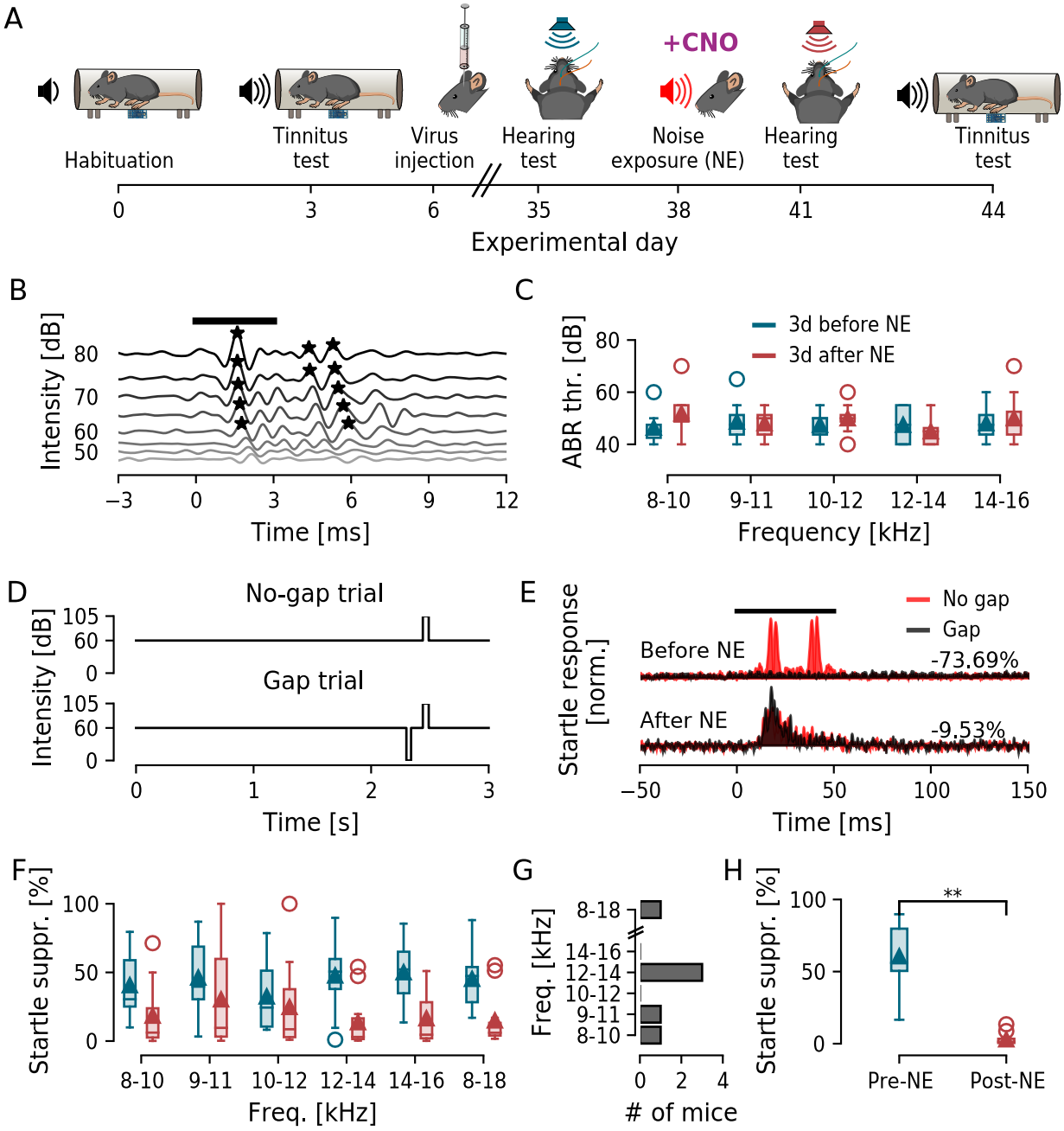

Figure 4: Inhibition of DCN CaMKIIα-hM4Di positive cells activity during noise exposure do not prevent tinnitus-like behaviour. A) Timeline of experiments for hearing threshold and GPIAS recordings. B-C) Representative ABR traces and group responses for mice that received i.p. CNO injection during noise exposure. D) Schematic outline of gap and no-gap protocols. E) Representative GPIAS response. F) Group results for startle suppression of all frequencies tested before (blue) and after (dark red) noise exposure in the presence of CNO. G) Quantification of most affected frequency of each animal. H) Startle suppression of animals receiving CNO during noise exposure shows tinnitus-like behavior 12 days after noise exposure. **: $P < 0.005$

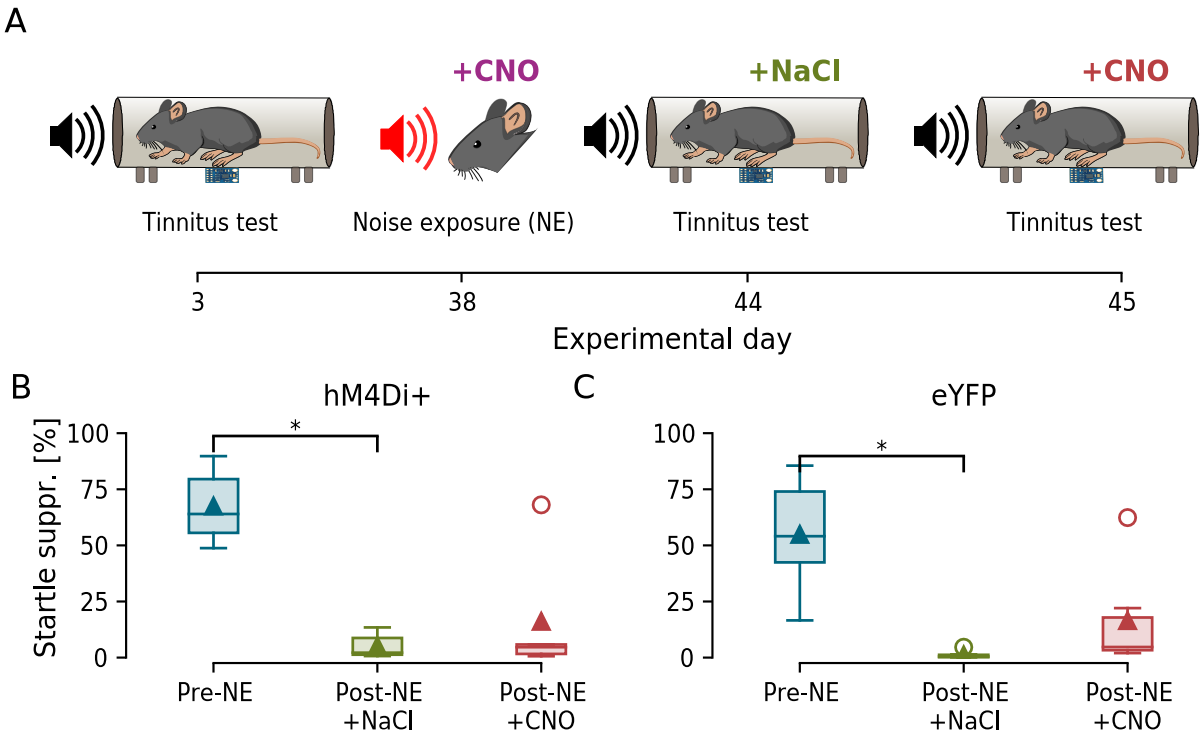

Figure 5: Decreasing CaMKIIα-hM4Di positive DCN cells activity during noise exposure abolish hM4Di-dependent recovery. A) Schematic timeline of GPIAS recordings. B) Inhibition of CaMKIIα-hM4Di positive DCN cells during noise exposure did not prevent a decrease in the startle suppression value, indicating tinnitus (n = 6 mice), and also CNO injection during GPIAS recording after noise exposure did not recover mice startle supression ($p = 0.482$). C) The control group (mice expressing eYFP) showed tinnitus-like behaviour after noise exposure (n = 6 mice) and did not recover the startle supression after CNO injection ($p = 0.175$). *: $p < 0.05$.

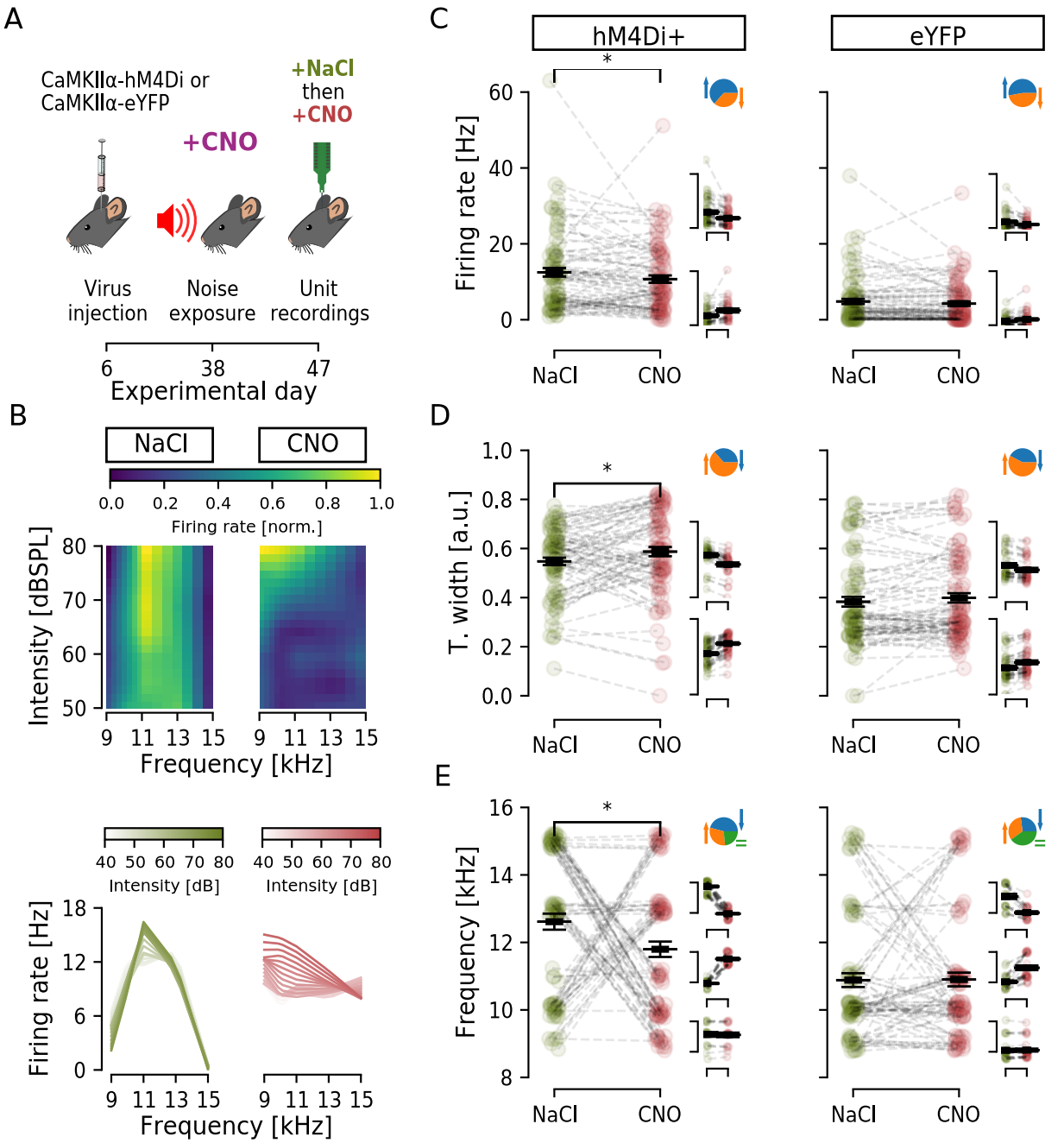

Figure 6: Decreasing activity of CaMKIIα-hM4Di positive DCN cells that were also inhibited during noise exposure changes firing properties of the circuitry. A) Timeline of experiments highlighting time of viral injection, noise exposure with CNO i.p. injection and unit recordings. B) Top, firing rate (colormap) of a representative unit after NaCl (left) and CNO (right) injection for each intensity (lines) and each frequency (columns) tested. Bottom, a different representation of the same representative examples in the top, showing firing rate per frequency for each intensity. C-E) Units firing rate (C), tuning width (D) and best frequency (E) for stimulation at 80dBSPL, at each unit best frequency. Left, 85 units from mice expressing hM4Di (n = 6 mice), showing significant difference after CNO application for Firing rate, Tuning width and Best frequency. Individual unit values are shown in green (NaCl) or red (CNO) condition. Black line indicates mean ± SEM. Right column, 91 units from mice expressing control eYFP (n = 6 mice), no significant difference. Insets show proportion of units decreasing (blue) or increasing (orange) parameters of each graph (see Suppl. Figure S2 for greater detail). *: $p < 0.05$.

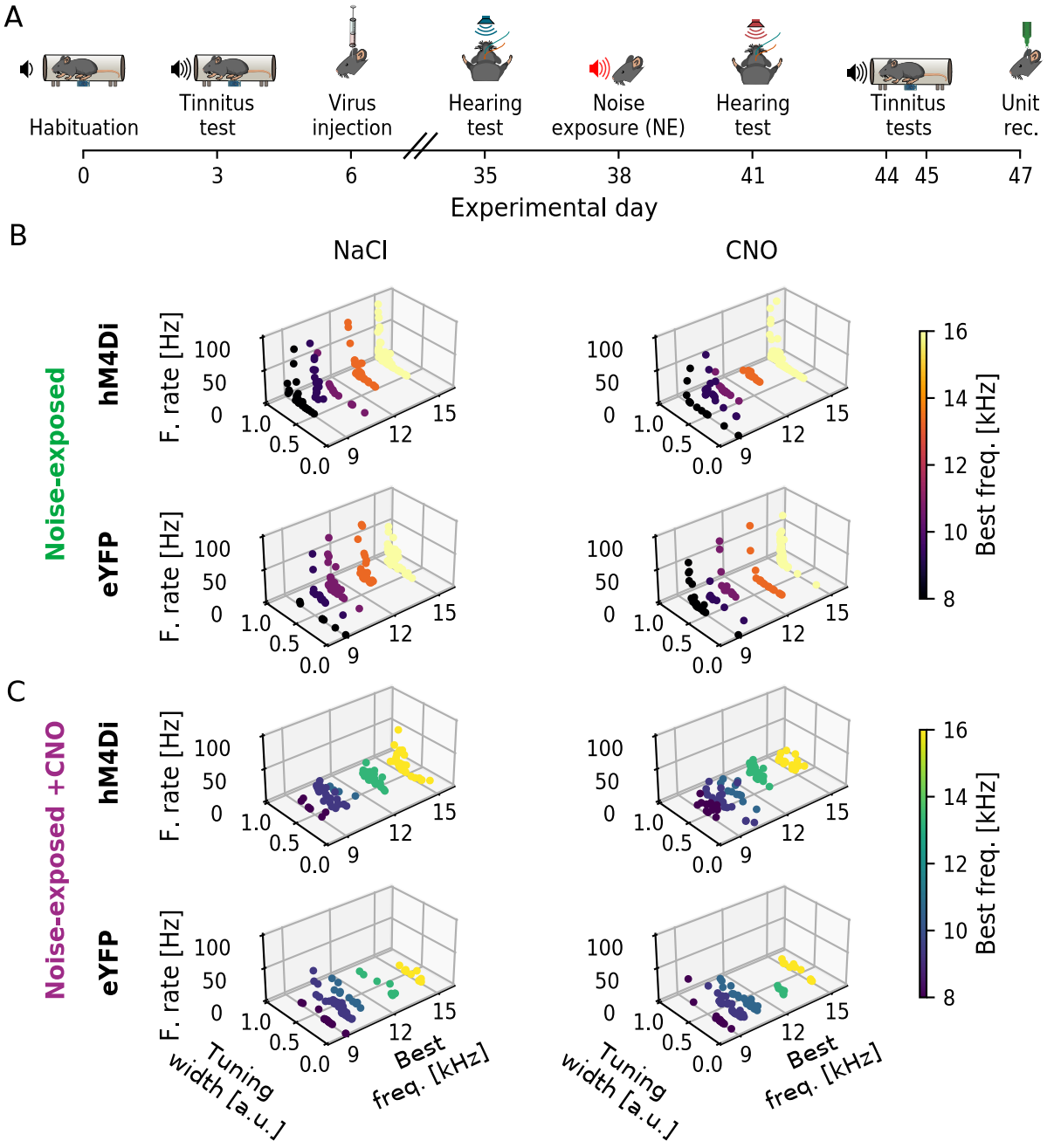

Figure 7: Three-dimensional scatters plots of Firing rate, Tuning width and Best frequency of DCN units of noise exposed hM4Di+ or eYFP+ animals in the presence of NaCl or CNO. A) Full experimental timeline. B) 3D scatters representing each unit by *firing rate x tuning width x best frequency* for hM4Di (experimental; top) and eYFP (control; bottom) animals under NaCl (left) or CNO (right) treatment. C) Same as B for experiments where animals were administered CNO (0.5mg/kg) 30 minutes prior to unit recordings. Colors represent the best frequency response between 8-16kHz.

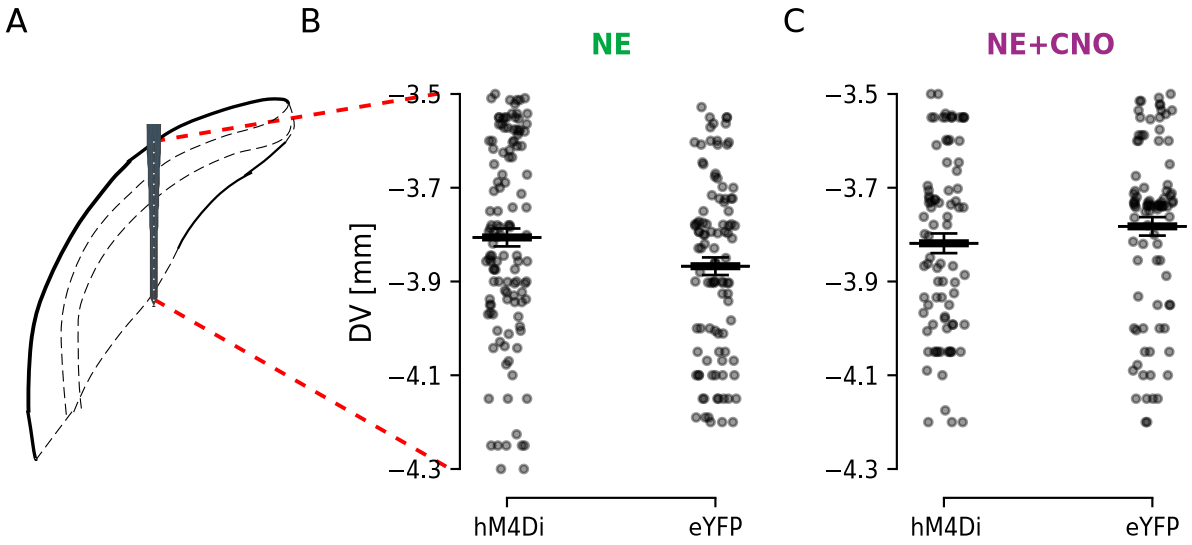

Figure 8: DCN unit depth profile. A) Schematic representation of the probe location within the DCN according to coordinates used highlighting the dorsoventral depth of unit recordings. B) Distribution of recorded DCN units along the dorsoventral axis for noise exposed animals expressing CaMKIIα-hM4Di or CaMKIIα-eYFP. C) The same as B but for experimental and control animals that were pre-treated with CNO 30 minutes before noise exposure. Black bars indicate mean ± SEM.